Appendix A to chapter 3 in the book
Development of Packaging and Products for Use in Microwave Ovens, 2020

⬡⬡⬡⬡⬡⬡⬡⬡⬡⬡
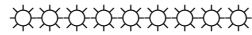
Analytical calculations for arbitrary rectangular microwave oven modes

Note: Equation numbers without a preceding A. refer to the book chapter.

A.1 Coupling factor and system matching

Since the upper (ceiling) and lower (bottom) ends of the oven cavity are closed by metal, the load is near the bottom, and the cavity height is larger than λ_0, one can analyse the system by assuming that the waves propagate downwards and are reflected upwards, setting up a standing wave pattern in the vertical direction. These patterns are thus principally determined by the same criteria as those in the horizontal directions. The load is now considered to be a flat horizontal slab covering the whole horizontal cross section. If this full surface coverage by the load not the case, no analytical calculations are possible and numerical modelling has to be carried out. However and quite importantly, it can be shown by numerical modelling that most of the mode characteristics obtained by the calculations described here apply quite well also for a "shelf coverage" by a slab-sheped load of 50 % or even less of the surface area.

Fig. A.1 Cavity feed and stationary signals

The energy input is now assumed to be in the cavity ceiling, but other locations are also possible to employ, then with the complication that hybrid modes become analytically more complicated to deal with. It can be shown that only a small coupling aperture is needed; see e.g. Paoloni [1989], then resulting in most of the retro-reflected energy from the slab load being reflected back downwards. The impedance transformation at the aperture makes system matching possible even for highly resonant modes and also provides mode selection by the aperture position and size. Slot apertures are dealt with by Harrington [1961]. The ceiling area is thus partially a reflector for the returning wave and partially an aperture that allows power to flow into the the cavity and also back into the feeding transmission line.

The analytical scenario is illustrated in Fig. A.1. The stationary input signal C_1^+ into the cavity is normalised to 1, but since the matching conditions at the aperture are not the same at the beginning of the energising as under stationary conditions, the cavity input signal with the transmission line signal as reference will gradually approach the stationary value – be it a constructive resonance or destructive interference or anything in between.

The reflection factor r^- is the electric field reflection factor at the load interface, and the minus superscript is for the upwards-propagating direction away from the load. It is determined by the general formula

$$r^- = \frac{\eta_L - \eta}{\eta_L + \eta} \qquad\qquad [A.1]$$

where η is the wave impedance of the cavity volume mode under study according to Eqs 3.6, and η_L the wave impedance of this mode inside the load. If the load ε is complex, r^- also becomes complex. However, the spatial phase of r^- due to the distance ℓ between the load an the reference plane at the ceiling and aperture must also be included as $e^{-jk\ell}$, where k is the cavity mode z-directed wavenumber k_z, obtained from

$$k_z{}^2 = \left(\frac{2\pi}{\lambda_0}\right)^2 - \left(\frac{m\pi}{a}\right)^2 - \left(\frac{n\pi}{b}\right)^2 \qquad\qquad [A.2]$$

No significant error is typically introduced by using $|\eta_L|$ with typical food materials since their $\varepsilon''/\varepsilon' = \tan\delta$ is less than about $\frac{1}{2}$.
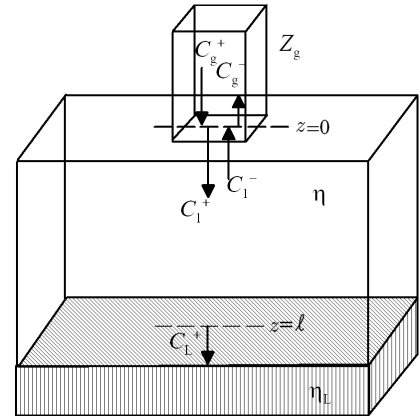
The characteristic impedance of the transmission line between the generator and the cavity is Z_g. The quotient C_g^-/C_g^+ is the transmission line reflection factor Γ. The quotient C_1^-/C_1^+ is the cavity load reflection factor r^- and refers to the reference plane in the cavity ceiling.

It is common not to make a distinction between transmission line and wave propagation quantities in descriptions of systems such as that under study here. Matching of both are needed in the junction. Different notation is therefore recommended for transmission lines (Z and Γ) and wave quantities (η and r). The boundary conditions for voltage and current in the port plane then give

$$C_g^+(1+\Gamma) = C_1^+(1+r^-) \qquad \text{(voltage and E field)} \qquad [A.3a]$$

$$C_g^+(1-\Gamma)/Z_g = C_1^+(1+r^-)/\eta \qquad \text{(current and H field)} \qquad [A.3b]$$

It is convenient to label the quotient

$$Z_g/\eta \equiv \varkappa_g \equiv \varkappa \qquad [A.4]$$

where $\varkappa$ is the important parameter *coupling impedance ratio* in cavity studies.

The aperture reflection factor r^+ as seen from the cavity is thus

$$r^+ = (Z_g - \eta)/(Z_g + \eta) = (\varkappa - 1)/(\varkappa + 1) \qquad [A.5]$$

There is another important parameter as well, which is intimately related to the system matching: the *(load) coupling factor χ*. It is defined as

$$\chi_{g,L} \equiv \chi = Z_g/\eta_L \qquad [A.6]$$

The condition $0 < \chi < 1$ is called undercoupling, $\chi = 1$ critical (or matched) coupling, and $\chi > 1$ is called overcoupling.

It is assumed here that Z_g is approximately real, since the cavity is fed directly by a lossless transmission line. Since η is also real, $\varkappa$ is also approximately real. If the cavity is fed by a very small aperture, $Z_g \to 0$. At system matched resonance (subscript R) one obtains, by insertion of Eq. A.1 into Eqs A.3:

$$Z_g = \eta_L \qquad \chi = 1 \qquad r^+ = r^- = r_R \qquad \varkappa_R = (1+r_R)/(1-r_R) \qquad \text{(matching at resonance)} \qquad [A.7]$$

A.2 Single mode system matching and Γ relationships for varying input

The frequency dependence of the stationary $\Gamma = C_g^-/C_g^+$ can be used as a practically relevant output variable for determination of frequency bandwidth and other data or example by a standard polar chart. $\varkappa_R$ is then firstly calculated and Z_g is then considered constant in the following calculations. By solving Eqs A.3 for Γ in a suitable frequency band one obtains

$$\Gamma = [1+r^- - \varkappa_R(1+r^-)]/[1+r^- + \varkappa_R(1+r^-)] \qquad [A.8]$$

The r^- refers to the horizontal E_{hor} field in the cavity ceiling and becomes negative real at TE mode resonance. A sign change is made when the calculations use the H_{hor} field as reference; that is the case for TM modes. For these, the sign of r^- changes when v passes the Brewster value v_B; the modified r^- thus becomes $+1$ for $v = 1$.

Since $v \cdot f$ is constant and equals the 'cut-off' frequency f_c, v must be varied for maintaining constant cavity geometry under frequency change. Of course, the frequency dependence of v has to be used also in the relationships for k_z and the recalculations of r^-. Insertion of the impedance relationships in Eqs 3.6 in to the definition of $\varkappa$ in Eq. A.4 gives, with $\varepsilon = 1$ in the cavity space

$$\varkappa^2 = \varkappa_R^2 \cdot (1-v^2)/(1-v_R^2) \qquad \text{(TEz modes)} \qquad [A.9a]$$

$$\varkappa^2 = \varkappa_R^2 \cdot (1-v_R^2)/(1-v^2) \qquad \text{(TMz modes)} \qquad [A.9b]$$

There is a mathemathical singularity for $v = 1$, since r^- becomes exactly -1 irrespectively of system dimensions, for both TE and TM. However, Γ is continuous at $v = 1$ so one just has to avoid that value in the numerical calculations.

A.3 Decomposition of TEx modes into TEz and TMz modes

With the load surface in a constant z plane, a pure TEx (i.e. TE to x) mode will no longer propagate as that after traversing the surface. Intuitively, that becomes obvious when the H field there is studied: it has x- and y-directed components and the latter must induce an x-directed current component in the dielectric load. This current is accompanied by a likewise x-directed E component, resulting in a violation of the TEx mode

characteristics.

What happens can be understood by decomposing the TE$_{mn}$x into a TE$_{mn}$z and TM$_{mn}$z mode. For unidirectional propagation, the mode amplitudes C_{TE} and C_{TM} must be such that the condition $E_x=0$ is achieved. Since C for TM modes is for the H field, the factor η_0 in the expression for C_{TM} dissapers when the E field is made reference as it is for C_{TE}. It follows that $E_{xTMz} + E_{xTEz} = 0$ and $E_{yTMz} + E_{yTEz} = E_{yTEx}$. Using Eqs 3.6 with the amplitude factors C as reference one obtains

$$C_{TEmn} = C_{TMmn} \cdot mb/na \cdot \sqrt{1-v^2} \qquad \text{(TE}_{mn}x \text{ mode)} \qquad \text{[A.10]}$$

The condition $E_x = 0$ in the aperture plane is maintained, which makes it necessary to use the sums $(C_{TE}{}^+ + C_{TE}{}^-)$ and $(C_{TM}{}^+ + C_{TM}{}^-)$. The orthogonality between the TE$_{mn}$z and TM$_{mn}$z modes is maintained, but their relative amplitudes and phases are determined by the cavity excitation and reflection factors at the load. The normalised power absorption in the load by the two modes becomes orthogonal in terms of the overall power. However, the heating pattern will be determined by the vectorially added fields.

A.4 Evanescent mode degeneracy

When $v > 1$, the orthogonality between the forward and backward waves in the cavity disappears. This seems not to be pointed out much in the literature, but can readily be shown by considering that the 'source' signal $C_1{}^+$ is reactive due to the imaginary factor $\sqrt{1-v^2}$ and the fact that orthogonality requires a sine or cosine variation which is replaced by exponential decay for evanescent modes; there is thus no phase which is needed for orthogonality.

By taking the Poynting vectors in the usual way, one obtaions the 'drastically' normalised power ($a = b = m = n = \lambda_0 = 1$):

$$P = \tfrac{1}{2}\sqrt{1-v^2} \cdot \left(1 - |r|^2\right) \qquad (v<1; \text{ TE and TM modes; } C^+=1) \qquad \text{[A.11a]}$$

$$P = \frac{1}{2}\operatorname{Re} S = \frac{1}{2}\operatorname{Re}\left[(1-r)\cdot\sqrt{1-v^2}\cdot(1+r)^*\right] \qquad (v>1; \text{ TM mode; } C^+=1) \qquad \text{[A.11b]}$$

$$P = \frac{1}{2}\operatorname{Re} S = \operatorname{Re}\frac{1}{2}\left[(1+r)\cdot\sqrt{1-v^2}\cdot(1-r)^*\right] \qquad (v>1; \text{ TE mode; } C^+=1) \qquad \text{[A.11c]}$$

where * is the complex conjugate. Note that an imaginary $\sqrt{1-v^2}$ is negative, due to the decay with distance.

A.5 Load power of aperture-fed cavity TM and TE modes

Since the E_y component is that which determines the mode amplitudes, the conditions for the E field of this mode is used. The normalisation is the same as for Eqs A.11, except that $E_{y,mn}$ is now set to 1 for both TEz and TMz modes.

The Poynting vector for the propagating TM mode in Eq A11a becomes proportional to the square of the amplitude $(1-r)$ of the field, where r is calculated in the feed plane. The r becomes negative for v beyond the Brewster condition, since the H field is reference for TM modes in this section. Secondly, the input mode E field amplitude is also proportional to $\sqrt{1-v^2}$, so that this factor squared must also be included. One obtains the mode power normalised for an input TM mode E field amplitude set to 1 as

$$P_{mode} = \frac{1}{2}\frac{1-|r|^2}{|1-r|^2 \cdot \sqrt{1-v^2}} \qquad (v < 1; \text{ TM mode; } E_{hor}=1) \qquad \text{[A.12a]}$$

When $v > 1$, the only difference is that the nominator is replaced by the expression in Eq. A.11b. Since reduction by $\sqrt{1-v^2}$ cannot now be made, one obtains

$$P_{mode} = \frac{1}{2}\frac{\operatorname{Re}\left[(1-r)\cdot\sqrt{1-v^2}\cdot(1+r)^*\right]}{|1-r|^2 \cdot \sqrt{1-v^2}} \qquad (v > 1; \text{ TM mode; } E_{hor}=1) \qquad \text{[A.12b]}$$

It is to be noted that P_{mode} represents what is possible to achieve in all possible cavities with any cross sections fulfilling the dimensional and free space wavelength criterion in Eq. 3.5, at a specified distance ℓ and with v as variable. The normalisation provides a true comparison for square cross section cavities with mode indices $m = n$ resulting in equal P_{mode} for $v = 0$.

It is of particular interest what P_{mode} is obtained for $\nu = 1$. For TM modes this is calculated by firstly setting the exponential factors $\exp(\pm jk_0\sqrt{1-\nu^2}z)$ to 1, representing either $z = 0$ or $\nu = 1$. After insertion in Eq. A12a and some manipulations one obtains, with the horizontal E field amplitude as reference:

$$P_{mode} = \frac{1}{2}\operatorname{Re}\frac{\varepsilon}{\sqrt{\varepsilon - 1}} \qquad (\nu = 1 \text{ and } \ell \text{ arbitrary; TM mode; } E_{hor}=1) \qquad [\text{A.13}]$$

Pseudo-Brewster TMz modes have $r \approx 0$. In a similar way as for the $\nu = 1$ case one obtains, with the Brewster condition in Eq. 3.1:

$$P_{mode} = \frac{1}{2}\operatorname{Re}\frac{\varepsilon}{\sqrt{\varepsilon - \nu_B}} = \frac{1}{2}\operatorname{Re}\sqrt{\varepsilon - 1} \qquad (\text{TM pseudo-Brewster mode; } E_{hor}=1) \qquad [\text{A.14}]$$

For the TEz modes a completely analogous derivation to that for TM modes gives the following

$$P_{mode} = \frac{1}{2}\frac{\left(1 - |r|^2\right)\cdot\sqrt{1 - \nu^2}}{|1 + r|^2} \qquad (\nu < 1; \text{ TE mode; } E_{hor}=1) \qquad [\text{A.15a}]$$

$$P_{mode} = \frac{1}{2}\frac{\operatorname{Re}\left[(1 + r)\cdot\sqrt{1 - \nu^2}\cdot(1 - r)^*\right]}{|1 + r|^2} \qquad (\nu > 1; \text{ TE mode; } E_{hor}=1) \qquad [\text{A.15b}]$$

Again, an imaginary $\sqrt{1-\nu^2}$ is negative. – By calculations as for the TM mode one finds that $P_{mode} \to 0$ for $\nu \to 1$. Amplitudes of evanescent TEz modes are thus insignificant, as shown in Fig. 3.10.

References

Harrington R.F. (1961) *Time-harmonic electromagnetic fields*, McGraw-Hill; section 8-15.

———————————